Journal of Qassim University for Science
2024, *Vol 3* (Issue 1), pp. 144-156
Received: 02 February 2024
Revised: 22 February 2024
Accepted: 29 February 2024

JQUS

Resonant Tunneling of Electrons and Holes through the AlGaAs/GaAsBi/AlGaAs Quantum Structure

Khulud Mohsen Rajan Aldhafeeri
Department of physics, College of Science, Qassim University, Burydah, Saudi Arabia, E-mail
Khalid336699@hotmail.com
Ahmed Rebey*
Department of physics, College of Science, Qassim University, Burydah, Saudi Arabia, E-mail
Ahmedrebey2@gmail.com

Abstract: In this paper, we report a quantitative study of a resonant tunneling diode (RTD) based on the AlGaAs/GaAsBi/AlGaAs structure as an active part of the device. First, the physical parameters of the GaAsBi alloy (bandgap energy, effective masses), to be used as input data for the calculation of transmission tunneling through the diode, are determined using the band anticrossing (BAC) approach. Second, we have calculated the I-V characteristic of RTD in order to analyze its performance via the values of peak-to-valley current ratio (PVCR) and negative differential conductance (NDC). Our calculation takes into account the effect of two types of carriers (electrons and holes) on the transport properties of the system. Remarkably, high performance (PVCR~450) is reached by optimizing the metallurgic and physical parameters of the structure. It is demonstrating that the incorporation of Bi in the GaAs matrix favors transport by holes and enhances the performance of RTD compared with standard one using electron conduction.

Keywords: GaAs/AlGaAs/GaAsBi structure, Resonant Tunneling Diode, Peak to valley current ratio, negative differential conductance.

1. Introduction

Early in the seventies, when the idea of superlattices had just been floated, Tsu and Esaki observed that resonant tunneling is a particular phenomenon in quantum wells [1, 2]. With its potential to produce a negative differential resistance (NDR) and THz operational capabilities, resonant tunneling has great promise for a diversity of applications. It has been explored experimentally and theoretically for several quantum systems [3-7]. The simple prototype is designed based on double-barrier semiconductor materials sandwiching the well. The physical properties of a resonant tunneling diode (RTD) depend on the nature and metallurgic design of the different elements of the structure. The performance of RTD is usually defined as the ratio of the peak current to the valley, denoted PVCR (peak to valley current ratio), extracted from the I-V characteristic. Complementary other indicators can also be defined to illustrate the characteristics of the diode, such as speed index, negative differential conductance (NDC), and time transit. The standard used structures are GaAs/AlAs, InGaAs/AlGaAs, and Si/SiGe, characterized by maximum PVCRs of 21.7, 35, and 2.9 [8-10], respectively. Depending on the intrinsic parameters (direct or indirect bangap, isotropy or anisotropy

of effective masses) of the operated material, the prediction of the transport properties of these diodes exhibits varying degrees of complexity. Evidently, the quality of the device requires other experimental restrictions to reduce defects such as mismatches and the possibility of doping during elaboration. Recently, the rapid advance of molecular beam epitaxy (MBE) and metalorganic chemical vapor deposition (MOCVD) as sophisticated epitaxial techniques has led to an innovative generation of structures based on the production of the new materials. III-V basic and compounds semiconductors structures are in expansion exploration in this research area. The choice of such material for any application is related to its particularity, such as the facility to be grown with a huge range of compositions or the existence of permanent polarization without any externally applied electric field. In spite of the several difficulties of realization, the investment in this way is of future interest. More recently, in order to reach high-performance of devices, some essays have focused on exotic quantum structures such as diluted magnetic semiconductors AlGaAs/GaMnAs [11, 12] and diluted mismatched semiconductors AlGaAs/GaAsBiN [13, 14]. The choice of these materials is founded on two fundamental motivations: the incorporation of Mn, N, or Bi in the GaAs matrix gives rise to (1) restructuration of energy bands and (2) spintronic applications due to the magnetic properties of the substituted atom. In fact, it is demonstrated that the incorporation of Bi in GaAs introduces a resonant energy level (E_{Bi}) in the valence band, which induces important effects on the physical properties of the mismatched alloy GaAsBi. The nomination mismatch is related to the difference between the electronegativity of As and Bi atoms. The experimental and theoretical qualification of this material is part of the expertise process. On the other hand, it was reported that the association of GaAsBi (well) with AlGaAs (barrier) has demonstrated a fascinating consequences and motivated results for its integration in several electronic and optoelectronic applications [15, 16, 17].

In this paper, we have explored the effect of Bi on the electron and hole transport properties of the AlGaAs/GaAsBi/AlGaAs double barrier structure as an active part of RTD. The results of I-V characteristics, PVCR, and NDC parameter calculations have been analyzed and discussed in comparison with the standard structure of AlGaAs/GaAs/AlGaAs.

2. Theoretical background:

We consider a RTD constituted by a double barrier AlGaAs and a central well GaAsBi.

The potential profile of the structure is described by

$$V(z) = \begin{cases} V(z), & m^* = m_b \text{ in the barrier} \\ 0\,, & m^* = m_w \text{ in the well} \end{cases} \qquad (1)$$

The widths of barrier and well are denoted L_b and L_w, respectively. Therefore, the width of all structure is L_s=2L_b+L_w. Our calculation concerns the electron and hole behaviors (the conduction and valence bands). In the case of holes, we take into account the splitting of the valence band, giving two types of effective masses: heavy holes (*hh*) and light holes (*lh*).

The recommended $Al_xGa_{1-x}As$ input parameters for resolution of Schrodinger equation are selected from literature. The aluminum composition range was chosen in order to explore the direct band gap nature of the material.

For a composition range of $\boldsymbol{0 \le x \le 0.45}$, the temperature and aluminum dependence of bandgap energy are given by [18]:

$$\boldsymbol{E_g^{Al_xGa_{1-x}As}(x,T) = E_g^{Al_xGa_{1-x}As}(x,T=0) - \frac{\alpha(x)T^2}{T+\beta(x)}} \qquad (2)$$

$$\boldsymbol{E_g^{Al_xGa_{1-x}As}(x,T=0) = 1.523 + 1.23x \quad (eV)} \qquad (3)$$

$$\boldsymbol{\alpha(x) = \left(5.5 + 3.35x + 50x^2\right) \times 10^{-4} \quad \left(\frac{eV}{K}\right)} \qquad (4)$$

$$\boldsymbol{\beta(x) = 198 + 88x + 4300x^2 \qquad (K)} \qquad (5)$$

$\boldsymbol{V_o = \Delta E_c^{AlGaAs/GaAs}}$ or $\boldsymbol{V_o = \Delta E_v^{AlGaAs/GaAs}}$ is the barrier height which measure the band offset in AlGaAs/GaAs junction. The value of $\boldsymbol{V_o}$ is determined using [19]:

$$V_o = \Delta E_c^{AlGaAs/GaAs} = 0.79\left(E_g^{AlGaAs} - E_g^{GaAs}\right) \qquad (6)$$

$$V_o = \Delta E_v^{AlGaAs/GaAs} = 0.46\left(E_g^{AlGaAs} - E_g^{GaAs}\right) \qquad (7)$$

The electron and hole effective masses are given by [20]

$$m_e^{AlGaAs}(x) = (0.067 + 0.083x)m_o \qquad (8)$$

$$m_{hh}^{AlGaAs}(x) = (0.51 + 0.25x)m_o \qquad (9)$$

$$m_{lh}^{AlGaAs}(x) = (0.082 + 0.068x)m_o \qquad (10)$$

hh and *lh* mean heavy holes and light holes, respectively.

The physical parameters (bandgap and effective masses) of GaAsBi alloy are determined by the (14×14) Band Anti-Crossing model (BAC) [21] at the ambient temperature. The mathematical formulation of this calculation is based on *k.p* method approach using a perturbative correction. The basic idea explains the difference between alloys is related to the energetic position of iosoelectronic impurity in host matrix. In fact, the electronegativity and size of substituted atom fix the distance between the resonant level and extermum of band (CB or VB). The interaction between the permitted band and this localized level induces a reconstruction of band structure. The reinstatement gives rise to variations of bandgap energy and effective masses. The degree of difficulty depends on the number of considered bands and to considered interactions.

In our case, we interest to GaAsBi alloy where a resonant level is introduced in the bottom of valence band at $E_{Bi} = -0{,}4\ eV$. The second one is located at $E_{Bi-so} = -1{,}9\ eV$ two-fold degenerate and interacts with spin-orbit band. their interaction with valence band maximum conducts to new subbands E+ and E- resulting from subdivision of band. The hybridization process between *6p* localized sates of Bi and the valence band states doubles each permitted band (hh, lh or so) into two subbands.

Numerical determination of effective masses (m^*) is made from a basic definition given by

$$\frac{1}{m^*} = \frac{1}{\hbar^2}\frac{\partial^2 E(k)}{\partial k^2}\bigg|_{\Gamma(k=0)} \qquad (11)$$

As supported by several works [22, 23], the determined values are supposed insensitive to the fluctuation of the temperature.

The novel AlGaAs/GaAsBi structure is characterized by a band offset that integrates the contributions of GaAsBi and AlGaAs as

$$\Delta E_c^{AlGaAs/GaAsBi} = 0.79\left(E_g^{AlGaAs} - E_g^{GaAs}\right) + \left(E_g^{GaAs} - E_g^{GaAsBi}\right) \qquad (12)$$

$$\Delta E_v^{AlGaAs/GaAsBi} = 0.46\left(E_g^{AlGaAs} - E_g^{GaAs}\right) + \left(E_g^{GaAs} - E_g^{GaAsBi}\right) \qquad (13)$$

The structure is perturbed by the presence of an external electric field denoted $F = -\frac{V_a}{L_s}z$ derived from a voltage V_a.

The potential of the structure becomes

$$V(z) = \begin{cases} \Delta E_{c,v}^{AlGaAs/GaAsBi} - \dfrac{V_a}{L_s} z, & m^* = m_b \text{ in the barrier} \\ -\dfrac{V_a}{L_s} z\,, & m^* = m_w \text{ in the well} \end{cases} \quad (14)$$

The behavior of carriers (electrons or holes) through the heterostructure is described by the wavefunction ψ issuing from the resolution of the Schrödinger equation

$$-\frac{\hbar^2}{2m^*}\frac{\partial^2\psi}{\partial z^2} + (V(z) - eFz)\psi = E\psi \quad (15)$$

The equation can be reduced to a simple one

$$\frac{\partial^2\psi}{\partial z'^2} - z'\psi = 0 \quad (16)$$

where $z' = \left(\frac{2m^*}{\hbar^2}\right)^{\frac{1}{3}}\left[\frac{V-E}{(eF)^{\frac{2}{3}}} - (eF)^{\frac{1}{3}}z\right] = \frac{\alpha+\beta z}{\gamma}$, $\alpha = \frac{2m^*}{\hbar^2}(\mathrm{V} - E)$ and $\beta = \frac{2m^*}{\hbar^2}(-eF)$

The one-dimensional Schrödinger equation solution takes the form of a linear combination between Airy functions *Ai* and *Bi* depending on the region location of carriers.

$$\begin{aligned} &\psi(z') = \mathrm{A}_1\, Ai(z') + \mathrm{B}_1\, Bi(z') && \text{for } \mathrm{z} < 0 \\ &\psi(z') = \mathrm{A}_2\, Ai(z') + \mathrm{B}_2\, Bi(z') && \text{for } 0 < \mathrm{z} < \mathrm{L_b} \\ &\psi(z') = \mathrm{A}_3\, Ai(z') + \mathrm{B}_3\, Bi(z') && \text{for } L_\mathrm{b} < \mathrm{z} < \mathrm{L_w} + L_\mathrm{b} \\ &\psi(z') = \mathrm{A}_4\, Ai(z') + \mathrm{B}_4\, Bi(z') && \text{for } \mathrm{L_w} + L_\mathrm{b} < \mathrm{z} < \mathrm{L_w} + 2L_\mathrm{b} \\ &\psi(z') = \mathrm{A}_5\, Ai(z') + \mathrm{B}_5\, Bi(z') && \text{for } \mathrm{L_w} + 2L_\mathrm{b} < \mathrm{z} \end{aligned} \quad (17)$$

By applying the boundary conditions at different interfaces of the structure, one can arrange a matrix relation between incident and transmitted waves as follows:

$$\begin{pmatrix} A_1 \\ B_1 \end{pmatrix} = [M]\begin{pmatrix} A_5 \\ B_5 \end{pmatrix} \quad (18)$$

Where $M = (M_1^{\square})^{-1}M_2^{\square}(M_3^{\square})^{-1}M_4^{\square}(M_5^{\square})^{-1}M_6^{\square}(M_7^{\square})^{-1}M_8^{\square}$ (19)

$$\begin{aligned} M_1^{\square}\begin{pmatrix} A_1 \\ B_1 \end{pmatrix} &= M_2^{\square}\begin{pmatrix} A_2 \\ B_2 \end{pmatrix} \\ M_3^{\square}\begin{pmatrix} A_2 \\ B_2 \end{pmatrix} &= M_4^{\square}\begin{pmatrix} A_3 \\ B_3 \end{pmatrix} \\ M_5^{\square}\begin{pmatrix} A_3 \\ B_3 \end{pmatrix} &= M_6^{\square}\begin{pmatrix} A_4 \\ B_4 \end{pmatrix} \\ M_7^{\square}\begin{pmatrix} A_4 \\ B_4 \end{pmatrix} &= M_8^{\square}\begin{pmatrix} A_5 \\ B_5 \end{pmatrix} \end{aligned} \quad (20)$$

Assuming there is no reflection in the exit part of the structure, that means that the coefficient B_5 must be zero.

$$\begin{pmatrix} A_1 \\ B_1 \end{pmatrix} = [M]\begin{pmatrix} A_5 \\ 0 \end{pmatrix} \quad (21)$$

$$A_1 = M_{11}A_5 \quad (22)$$

Finally, the transmission is given by the ratio

$$\tau(\varepsilon) = \frac{A_5A_5^*}{A_1A_1^*} = \frac{1}{M_{11}(M_{11})^*} \quad (23)$$

Where ε is the incident energy.

The current density J is calculated using the integral [1, 2]:

$$J = \frac{em_ok_BT}{2\pi^2\hbar^3}\int_0^{+\infty}\frac{k_5}{k_1}\tau(\varepsilon).\tau(\varepsilon)^* ln\left[\frac{1+\exp\left(\frac{E_F-\varepsilon}{k_BT}\right)}{1+\exp\left(\frac{E_F-\varepsilon-eV_a}{k_BT}\right)}\right]d\varepsilon \quad (24)$$

$k_1^2 = \frac{2m_{GaAs}}{\hbar^2}\varepsilon$, $k_5^2 = \frac{2m_{GaAs}}{\hbar^2}(\varepsilon + eV_a)$

E_F is the Fermi level, and T is the temperature.

3. Results and discussion

In this study, the dimension of the structure (L_w, L_b) has a vital importance. Indeed, the width of the well should ensure the confinement of electron. Therefore, it's important to restrict the limit values of this parameter. A particular interest should be given to the maximum width of the well (L_{wmax}). Its expression is estimated from the fundamental energy levels equation in the quantum well

$$\left|\cos\left(\sqrt{\frac{2m_wE}{\hbar^2}}L_w\right)\right| = \sqrt{\frac{m_bE}{m_bE + m_w(V_0 - E)}} \qquad (25)$$

By replacing the energy E by the thermal energy (de Broglie wavelength)$E_{th}(\lambda_{th})$ [24]

$$L_{wmax} = \frac{\lambda_{th}}{2\sqrt{\pi}}cos^{-1}\left(\sqrt{\frac{E_{th}}{E_{th}\left(1 - \frac{m_w}{m_b}\right) + \frac{m_w}{m_b}(V_0)}}\right) \qquad (26)$$

The physical sense of L_{wmax} arises from the fact that the energy of the fundamental levels in the QW well must be larger than thermal energy.

Figure 1 shows a schematic illustration of the considered AlGaAs/GaAsBi/AlGaAs double barrier structure. We report on the same figure the calculated electronic energy levels and the correspondent wavefunctions for a symmetric structure. This calculation is processed by a subroutine based on the discretization of the Schrodinger equation. Indeed, The Schrödinger equation is solved using a variable optimized mesh and the error on the energy levels is estimated to about 5×10^{-4}. The structure shows two confined levels E_1 and E_2 with symmetric and asymmetric wavefunctions, respectively.

Using the same parameters as in figure 1, we have calculated the transmittance of the electron carriers through this system. As reported in Figure 2, transmittance reveals the existence of two sharp peaks located at E_1 and E_2. Above the V_o value, the transmittance curves show oscillations. These energy levels depend on the physical parameters of the structure, such as L_w, L_b, V_o, m_b, and m_w. Experimentally, L_w and L_b are metallurgic parameters and would be fixed during the growth. However, V_o, m_b, and m_w are intrinsic physical parameters changed by varying the chemical composition of the well and barrier alloys. In our case, the parameters of the AlGaAs barrier are governed by the change in aluminum composition; however, the parameters of the GaAsBi well are varied by the modification of bismuth composition. Also, an external applied voltage, V_a, can be applied to the structure to be in forward or inverse polarization. The range of this voltage depends on the structure and nature of application. Figure 3 shows the effect of the external voltage on the transmission variation with energy. An increase in V_a shifts all peaks to the low energies. This result is in good agreement with the literature [13, 25].

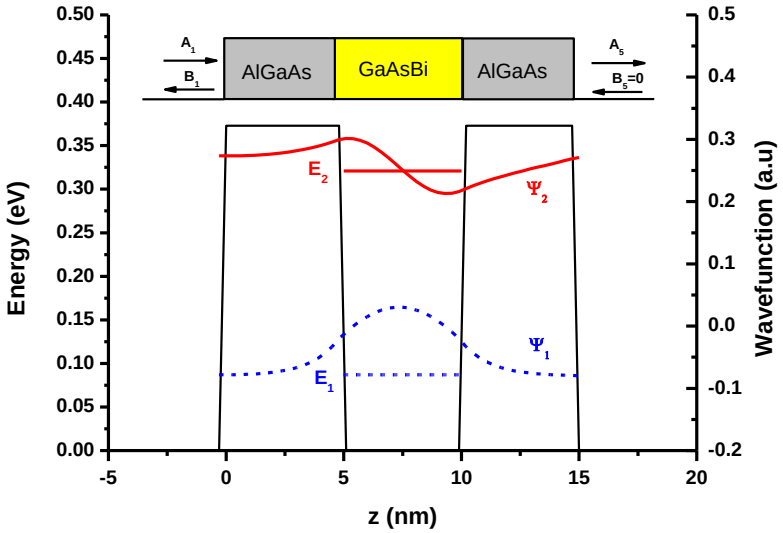

Figure 1: Schematic illustration of the considered AlGaAs/GaAsBi/AlGaAs double barrier structure $L_w=L_{B1}=L_{B2}=5nm$; $V_o=0.373eV$; $m_b=0.092m_o$ and $m_w=0.067m_o$. Left Y-axis: energy of confined levels in the well. Right Y-axis: wavefunctions of the two confined levels.

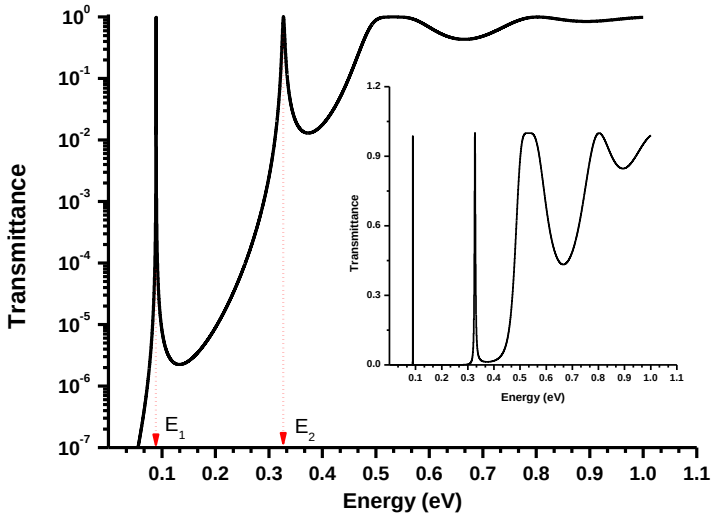

Figure 2: The logarithmic transmittance evolution versus energy for the considered AlGaAs/GaAsBi/AlGaAs double barrier structure $L_w=L_{B1}=L_{B2}=5nm$; $V_o=0.373eV$; $m_b=0.092m_o$ and $m_w=0.067m_o$. The inset shows a linear-scale representation of the transmittance curve.

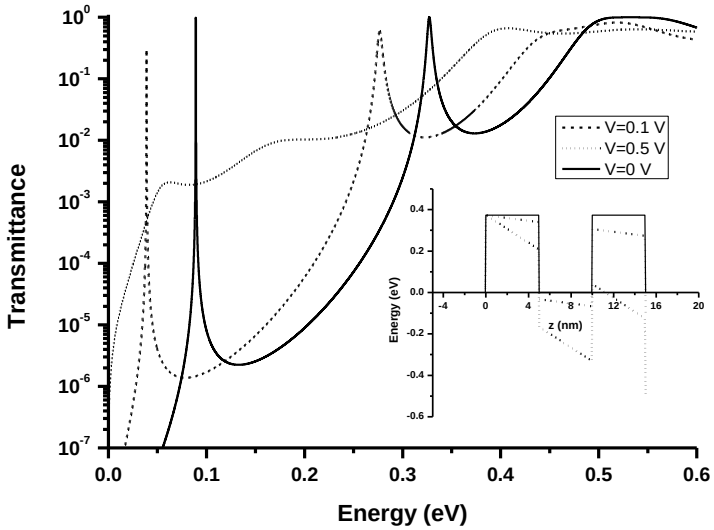

Figure 3: The logarithmic transmittance evolution versus energy for the considered AlGaAs/GaAsBi/AlGaAs double barrier structure $L_w=L_{B1}=L_{B2}=5nm$; $V_o=0.373eV$; $m_b=0.092m_o$ and $m_w=0.067m_o$. The inset shows the effect of V_a on the potential of the structure.

In this part, we focus our study on the performance of the RTD based on the AlGaAs/GaAsBi/AlGaAs compared to the standard AlGaAs/GaAs/AlGaAs diode. It is known that the incorporation of Bi in GaAs modifies the valence band structure behavior. Consequently, a particular interest will be given to the holes transport.

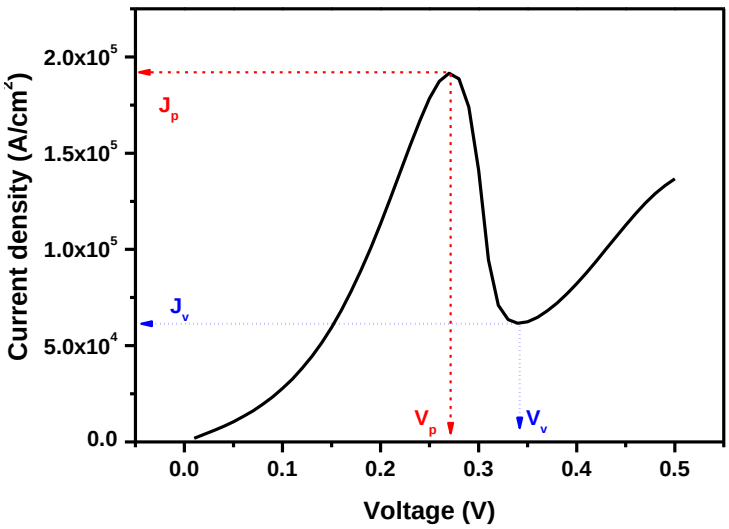

Figure 4: The calculated I-V characteristic shows the critical points to define PVCR and the differential resistance R_D.

In order to quantify the performance of a structure destined for RTD fabrication, we have calculated the PVCR indicator. Figure 4 illustrates the definition of PVCR as the ratio of peak current J_p and valley current J_v. Also, the differential resistance R_D and the conductance G are determined using the formula

$$\frac{1}{G} = R_D = \frac{J_p - J_v}{V_p - V_v} < 0$$

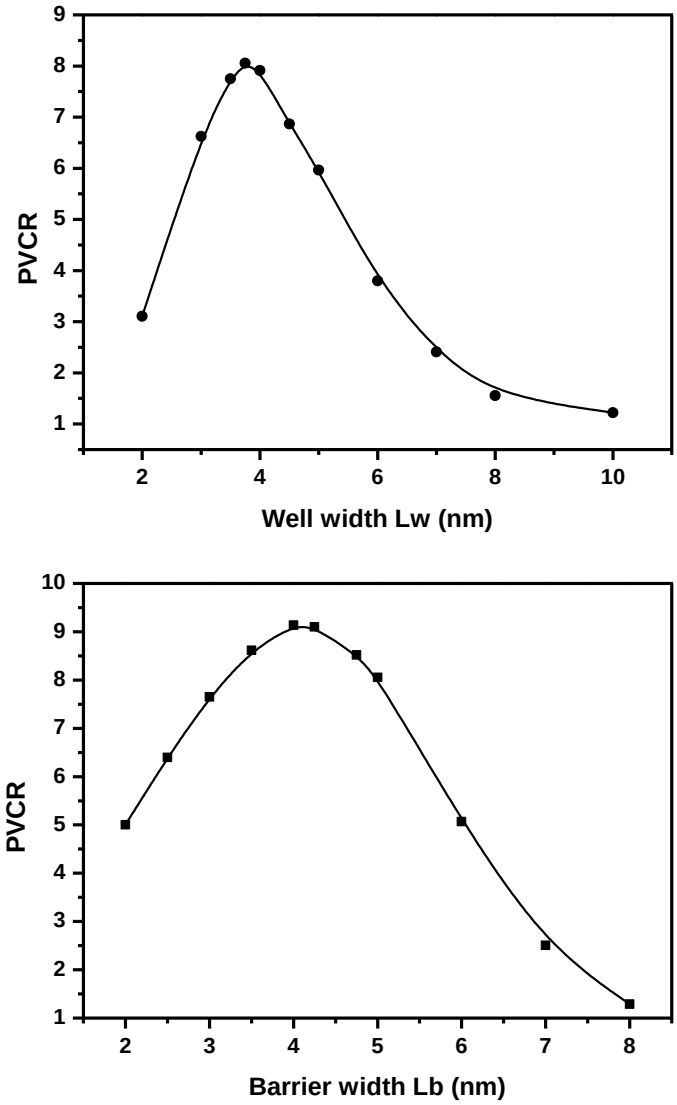

Figure 5: Calculated PVCR as a function of L_w and L_b for the standard $Al_{0.3}Ga_{0.7}As/GaAs/Al_{0.3}Ga_{0.7}As$ structure.

For the standard AlGaAs/GaAs/AlGaAs structure, we have calculated the PVCR when varying the well and the barrier widths. The results of this optimization are reported in Figure 5. The barrier height is taking constant supposed to correspond to an aluminum composition of 0.3. It is clearly noted that maximum PVCR is reached when choosing the couple (L_w=*3.75nm*, L_b=*4nm*). This value is 9.13 which is in good agreement with the maximum value reported experimentally for this type of diode [4, 8].

On the other hand, we have calculated the PVCR relative to the same diode but with hole transport. For this calculation, we have considered L_w=*3.75nm*, L_b=*4nm*, $V_o = \Delta E_v^{AlGaAs/GaAs}$ and the relative masses of light holes (m_{lh}^{AlGaAs}) and heavy holes (m_{hh}^{AlGaAs}).

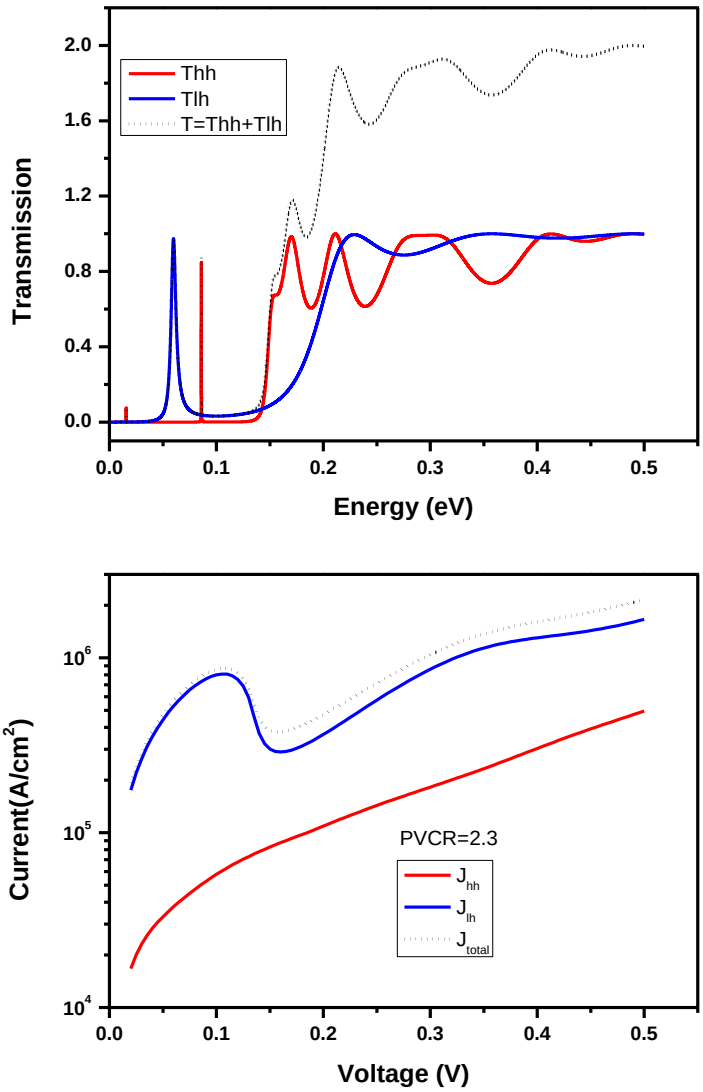

Figure 6: Transmission and current density curves were calculated for the valence band of the standard $Al_{0.3}Ga_{0.7}As/GaAs/Al_{0.3}Ga_{0.7}As$ structure.

As demonstrated by this calculation, a structure based on hole transport presents less performance (PVCR=2.30<9.13) compared to that using electrons. The transmission shows two behaviors due to the difference between the values of the effective masses of holes. The significative values of total transmission in the calculation of I-V characteristics are considered only for $E<V_o$. As expected, the total current is dominated by the light-hole current. In fact, the term of reduced mass holes $\mu = \frac{m_{lh}m_{hh}}{m_{lh}+m_{hh}} \approx m_{lh}$ contributes in the process of hole transport.

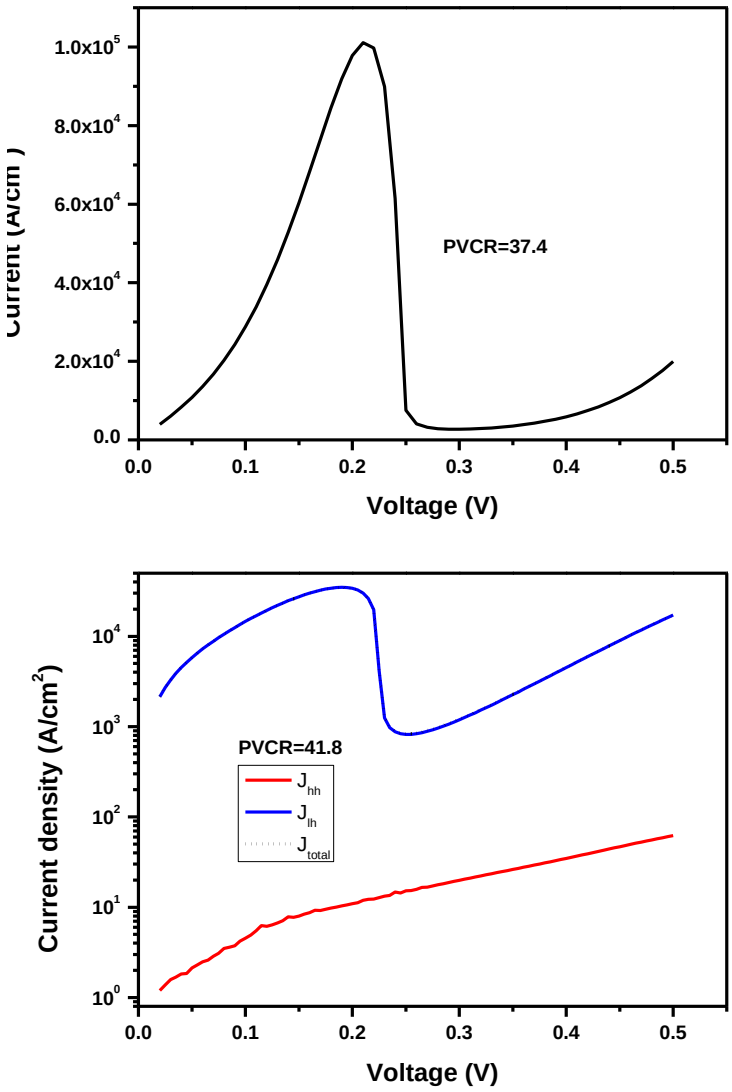

Figure 7: Transmission and current density curves were calculated for the valence band of the standard $Al_{0.3}Ga_{0.7}As/Ga\ As_{0.095}Bi_{0.05}/Al_{0.3}Ga_{0.7}As$ structure.

In order to enhance the performance of the diode, we have replaced the GaAs with GaAsBi material. The calculated I-V characteristics for electrons and holes taking the same metallurgic parameter (L_w=*3.75nm*, L_b=*4nm*) are given in figure 7 for a Bi composition of 5%. Clear enhancement of the performance of the diode not only for electron transport behavior but particularly for hole ones. This fact is related to the effect of Bi content on the physical properties of considered quantum well. Indeed, Bi introduces a resonant level (E_{Bi}) inside the valence band gives rise to a new arrangement of the band structure, which affects essentially the hole masses and reduces the bandgap energy. The conduction band is affected only by its coupling with the valence band. Any change in the composition can influence the transport properties of the structure. In figure 8, we report recapitulation results based on the calculation of PVCR and conductance of the diode as a function of Bi content. The Bi composition range is limited to 10%, where the applied BAC model is valuable in determining the physical properties of bulk GaAsBi alloys.

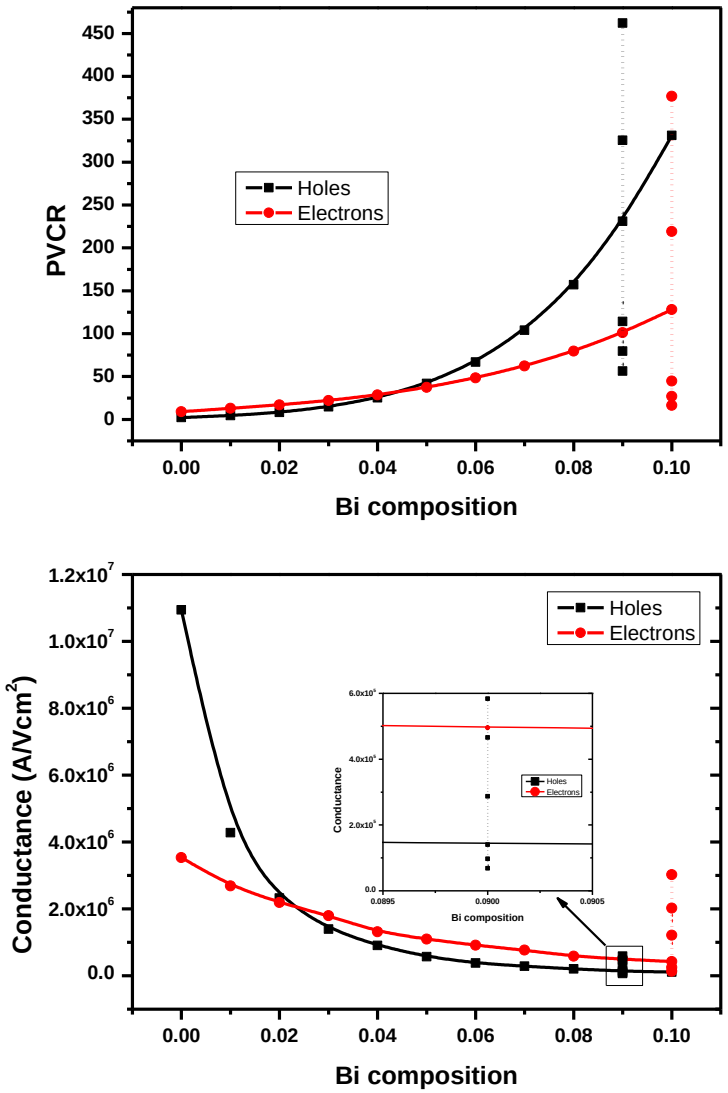

Figure 8: PVCR and conductance curves were calculated for holes and electrons as a function of Bi composition for $Al_{0.3}Ga_{0.7}As/GaAs_{1-x}Bi_x/Al_{0.3}Ga_{0.7}As$. The vertical curves are the results of the variation of V_o using aluminum composition and keeping Bi composition constant.

Remarkably, by adjusting the composition of Bi and aluminum, we can reach a high performance (~450) for the diode and reduce the conductance. The optimized diode shows high performance compared to those available in device applications such as AlGaAs/GaAs/AlGaAs, GaAs/InGaAsBi/GaAs, Si/SiGe/Si,…etc. It is also possible to enhance this performance by combining nitrades and bismide alloys. These results are of high interest and open the way to explore these alloys in device applications.

Conclusion:

A theoretical numerical formulation has been used to study the transport properties through the AlGaAs/GaAsBi/AlGaAs quantum structure. This system constitutes the active part of the resonant tunneling diode (RTD) device. In order to optimize the performance of RTD, the physical parameters of the GaAsBi alloy for different Bi contents are calculated based on the band anticrossing approach. A particular interest is given to the determination of the effective masses of electrons, and holes, and bandgap energies. These purposes serve as input parameters for the

resolution of the Schrodinger equation and the calculation of the tunneling transmission. The performance of the diode is determined by calculating the PVCR and NDC parameters when considering the electron or hole transport process. It should be noted that an increase in Bi composition enhances the PVCR and reduces the NDC values. This behavior is more appropriate when the transport is processed by holes. A high PCVR of about 450 is reached when combining mutually the Bi content and aluminum composition of the AlGaAs barrier. The proposed structure shows high performance compared to standard ones (AlGaAs/GaAs/AlGaAs, GaAs/InGaAsBi/GaAs, Si/SiGe/Si,…etc.) opening the way to its synthesis and exploring it in different THz device applications.

REFERENCES:

1. R. Tsu and L. Esaki, *Tunneling in a finite superlattice*, Appl. Phys. Lett., 22, 562-564, (1973).

2. L. Esaki, L. L. Chang, *New Transport Phenomenon in a Semiconductor Superlattice*, Phys. Rev. Lett. 33, 495 (1974).

3. J. Nanda, P. K. Mahapatra, C. L. Roy, *Transmission coefficient, resonant tunneling lifetime and traversal time in multibarrier semiconductor heterostructure*, Physica B 383, 232-242 (2006).

4. S. Ipsita, P. K. Mahapatra, P. Panchadhyayee, *Optimum device parameters to attain the highest peak to valley current ratio (PVCR) in resonant tunneling diodes (RTD)*, Physica B 611, 412788 (2021).

5. A. Rebey, M. Mbarki, H. Rebei, S. Messaoudi, *Performance optimization of AlGaAs/GaAsBiN resonant tunneling diode*, Optik 268, 169793 (2022).

6. S. Sankaranarayanan, D. Saha, *Giant peak to valley ratio in a GaN based resonant tunnel diode with barrier modulation*, superlattices and microstructures 98, 174-180 (2016).

7. I. Asennova, E. Valcheva, D. Arnaudov, *Tunnelling and current density in short period strained AlN/GaN superlattices*, Physica E 63,139-146 (2014).

8. C.I. Huang, M.J. Paulus, C.A. Bozada, S.C. Dudley, K.R. Evans, C.E. Stutz, M. E. Cheney, *AlGaAs/GaAs double-barrier diodes with a high peak-to-valley current ratio*, Appl. Phys. Lett. 51 (2), 121–123 (1987).

9. T. Inata, S. Muto, Y. Nakata, S. Sasa, T. Fujii, S. Hiyamizu, *A pseudomorphic In0.53Ga0.47As/AlAs resonant tunneling barrier with a peak-to-valley current ratio of 14 at room temperature*, Jpn. J. Appl. Phys. 26 (Part 2, No. 8), L1332–L1334 (1987).

10. P. See, D.J. Paul, B. Hollander, S. Mantl, I.V. Zozoulenko, K.-F. Berggren, *High performance Si/Si/sub 1-x/Gex resonant tunneling diodes*, IEEE Electron. Device Lett. 22 (4), 182–184 (2001).

11. H.-B. Wu,1 K. Chang,1 J.-B. Xia,1 and F. M. Peeters, *Resonant Tunneling of Holes in GaMnAs-Related Double-Barrier Structures*, Journal of Superconductivity: Incorporating Novel Magnetism, Vol. 16, No. 2, (2003).

12. S. Kerimova, O. Donmez, M. Gunes, F. Kuruoglu, M. Aydın, C. Gumus, A. Erol, *Analysis of mixed optical transitions in dilute magnetic AlAs/GaAs/GaAsMn quantum wells grown on high substrate index grown by molecular beam epitaxy*, Material science and engineering: B, Volume 290, 116349, (2023).

13. A. Rebey, M. Mbarki, H. Rebei, S. Messaoudi, *Tunneling in matched AlGaAs/GaAsBiN superlattices*, Applied Physics A 128 (5), 1-10 (2022).

14. K. Chakir, C. Bilel, M.M. Habchi, A. Rebey, *Discontinuities and bands alignments of strain-balanced III-VN/III-V-Bi heterojunctions for mid-infrared photodetectors*, Superlattices and Microstructures 102, 56-63 (2017) and references therein.

15. S. Pūkienė, M. Karaliūnas, A. Jasinskas, E. Dudutienė, B. Čechavičius, J. Devenson, R. Butkutė, A. Udal and G. Valušis, *Enhancement of photoluminescence of GaAsBi quantum wells by parabolic design of AlGaAs barriers*, *Nanotechnology* 30, 455001, (2019).

16. O. Donmez, M. Aydin, S. Ardali, S. Yildirim, E. Tiras, A. Erol, J. Puustinen, J. Hilska, M. Guina, *Power loss mechanisms in n-type modulation-doped AlGaAs/GaAsBi quantum well heterostructures*, Semicond. Sci. Technol. 35, 095038 (2020).

17. O. Donmez, M. Aydin, S. Ardali, S. Yildirim, E. Tiras, F. Nutku, C. Cetinkaya, E. Cokduygulular, J. Puustinen, J. Hilska, M. Guina, A. Erol, *Electronic transport in n-type modulation doped AlGaAs/GaAsBi quantum well structures: influence of Bi and thermal annealing on electron effective mass and electron mobility*, Semicond. Sci. Technol. 35, 025009 (2020).

18. S. A. Lourenc¸O, I. F. L. Dias, J. L. Duarte, and E. Laureto, E. A. Meneses, J. R. Leite, I. Mazzaro, *Temperature dependence of optical transitions in AlGaAs*, J. Appl. Phys., Vol. 89, No. 11, 6159- 6164 (2001).

19. Goldberg Yu.A. *Handbook Series on Semiconductor Parameters*, vol.2, M. Levinshtein, S. Rumyantsev and M. Shur, ed., World Scientific, London, 1-36 (1999).

20. Paul Harrison and Alex Valavanis, *Quantum Wells, Wires and Dots: Theoretical and Computational Physics of Semiconductor Nanostructures*, Fourth Edition, John Wiley & Sons, Ltd. Published (2016) by John Wiley & Sons, Ltd.

21. M. M. Habchi, A. B. Nasr, A. Rebey, B. El Jani, *Theoretical study of optoelectronic properties of GaAs1− xBix alloys using valence band anticrossing model*, Infrared Physics & Technology 67, 531-536 (2014).

22. M. Yoshimoto, W. Huang, G. feng, K. Oe, *New semiconductor alloy GaNAsBiN with temperature-insensitive bandgap*, Phys. Stat. sol (b) 243, No.7, 1421-1425 (2006).

23. W. Huang, K. Oe, G. Feng, M. Yoshimoto, *Molecular beam epitaxy characteristics of GaNAsBi*, J. Appl. Phys. 98, 053505 (2005).

24. D. Hestenes, *Quantum mechanics from self-interaction*, Foundations of Physics, 15, 63 (1985).

25. P. Panchadhyayee, R. Biswas, Arif Khan, and P. K. Mahapatra, *Electric-field-induced resonant tunneling lifetime in semiconductor multibarrier systems,* Journal of Applied Physics 104, 084517 (2008).